IL-21 signaling promotes early dissemination of KSHV infection in B lymphocytes

Nedaa Alomari[1], Farizeh Aalam[1], Romina Nabiee[1], Jesus Ramirez Castano[1] and Jennifer Totonchy‡

[1]Biomedical and Pharmaceutical Sciences, Chapman University, Irvine, CA USA

‡Corresponding Author

Jennifer Totonchy

Chapman University School of Pharmacy

9410 Jeronimo Road

Irvine, CA

Phone: 714-516-5438

Email: totonchy@chapman.edu

Short Title: IL-21 and KSHV infection of B cells

Abstract

Kaposi's sarcoma-associated herpesvirus (KSHV) extensively manipulates the host immune system and the cytokine milieu, and cytokines are known to influence the progression of KSHV-associated diseases. However, the precise role of cytokines in the early stages of KSHV infection remains undefined. Here, using our unique model of KSHV infection in tonsil lymphocytes, we investigate the influence of host cytokines on the establishment of KSHV infection in B cells. Our data demonstrate that KSHV manipulates the host cytokine microenvironment during early infection and susceptibility generally associated with downregulation of multiple cytokines. However, we show that IL-21 signaling promotes KSHV infection by promoting both plasma cell numbers and increasing KSHV infection in plasma cells. Our data reveal that IL-21 producing T cells, particularly Th17/Tc17 and central memory CD8+ T cells may represent immunological factors that modulate host-level susceptibility to KSHV infection. These results suggest that IL-21 plays a significant role in the early stages of KSHV infection in the human immune system and may represent a novel mechanism to be further explored in the context of preventing KSHV transmission.

Author Summary

Very little is known about how KSHV is transmitted and how it initially establishes infection in a new human host and this lack of information limits our ability to prevent KSHV-associated cancers by limiting its person-to-person transmission. Saliva is thought to be the primary route of person-to-person transmission for KSHV, making the tonsil a likely first site for KSHV replication in a new human host. In particular, the tonsil is likely to be the first place KSHV is able to enter B cells, which are thought to be a major site of persistent infection. Our previous work identified

plasma cells as a highly targeted cell type in early KSHV infection in cultured cells from human tonsil. In this study, we show that the human cytokine IL-21 promotes both overall KSHV infection and the establishment of infection in plasma cells. We also investigate the immunological mechanisms underlying this effect. Our results demonstrate that IL-21 and IL-21-producing cells are a novel factor that influences the initial establishment of KSHV infection in humans.

Introduction

Kaposi's Sarcoma Herpesvirus (KSHV) is a lymphotropic gamma-herpesvirus, originally discovered as the causative agent of Kaposi Sarcoma (KS) [1]. KS is a highly proliferative tumor derived from lymphatic endothelial cells [2]. KSHV is also associated with the B cell lymphoproliferative diseases, Primary Effusion Lymphoma (PEL) and Multicentric Castleman's Disease (MCD) [3, 4], as well as the inflammatory disorder KSHV inflammatory cytokine syndrome (KICS) [5]. KSHV is linked to 1% of all human tumors, and the World Health Organization (WHO) has classified it as class I carcinogen [6, 7]. KSHV infection is asymptomatic in most healthy individuals, and KSHV-associated malignancies arise primarily in immunocompromised patients. Indeed, KS remains one of the most common cancers in people living with HIV/AIDS [8].

The geographical distribution of KSHV is not ubiquitous. KSHV infection is endemic in sub-Saharan Africa and in the Mediterranean basin. KSHV prevalence is also high in subpopulations in other parts of the world such as men who have sex with men (MSM). Saliva is the only secretion where KSHV DNA is commonly detected [9], and, based on this, person-to-person transmission of KSHV is thought to occur via saliva. The oral lymphoid tissues are rich in KSHV target cell types including lymphatic endothelial cells and B cells, and are therefore a likely site for the initial

establishment of KSHV infection in a new human host. However, the exact mechanisms for KSHV transmission and how environmental, behavioral and host factors influence transmission and early infection events remain to be established. This gap in our understanding dramatically affects our ability to find efficient strategies to decrease the transmission or influence host-level susceptibility to KSHV infection. One of the main factors that has been linked to KSHV-associated lymphoproliferations is cytokine dysregulation [10]. However, their contribution to the early stages of KSHV infection and whether the cytokine milieu in the oral cavity contributes to host-level susceptibility to KSHV infection is unclear. KSHV-infected cells in KSHV-associated lymphoproliferative diseases generally display plasma cell or plasmablast features [11], and our recent work showed that KSHV targets plasma cells in early infection in tonsil B lymphocytes [12]. Whether the KSHV-infected plasma cells we observe arise from direct infection or differentiation from a precursor B cell subset remains to be established. In either case, it is likely that cytokines play a role in supporting the survival and/or differentiation of KSHV-infected plasma cells.

IL-21 is a pleiotropic cytokine that has diverse effects on B cell, T cell, macrophage, monocyte, and dendritic cell biology. It is produced mainly by natural killer T (NKT) cells and CD4+ T cells, including follicular helper (TFH) cells [13]. The IL-21 receptor is expressed by several immune cells, including B and T cells and is comprised of a unique IL-21R subunit and the common cytokine receptor γ chain (CD132), which is also part of the receptor for IL-2, IL-4, IL-7, IL-9, and IL-15 [14]. IL-21 plays a critical role in B cell activation and expansion [15], and plays a critical role in B cell differentiation to immunoglobulin (Ig)-secreting plasma cells. The regulation of maturation of B cells into plasma cell is driven by the several transcription factors including

Blimp1 and Bcl6 [16], which can both be induced by IL-21 signaling, indicating that IL-21 is an important regulator of plasma cell differentiation [17, 18].

There are few studies to date examining the contribution of IL-21 to KSHV infection and KSHV-associated disease. However, IL-21 is detected in interfollicular areas in MCD patients [19]. Moreover, IL-21 induces differentiation of B-lymphoblastoid cell lines (BCLs) into late plasmablasts/early plasma cells and regulates the expression of many latent proteins in EBV^{+} Burkitt lymphoma cell lines [20, 21]. Importantly, IL-21 signaling is required for the establishment of MHV-68 infection and the generation for MHV-68 infected long-lived plasma cells in mice [22].

In this study, we use our well-established tonsil lymphocyte infection model to explore whether KSHV alters cytokine secretion early in infection and whether cytokine levels have an effect on the establishment of KSHV infection. We identify IL-21 as a factor that specifically influences KSHV infection in plasma cells, which we previously characterized as a highly targeted cell type in early infection [12]. We demonstrate that IL-21 signaling increases plasma cell levels in our *ex vivo* model system and that this effect promotes overall KSHV infection. We explore the mechanisms of IL-21 signaling by establishing which B cell types are responding IL-21 and what T cell subsets are producing IL-21 in our model.

We determine that expression of IL-21 receptor (IL-21R) on naïve and classical memory T cells is correlated with increased KSHV infection in IL-21 treated cultures, and we demonstrate that both KSHV infection and IL-21 treatment modulates IL-21R expression on B cells. We examine IL-21 secretion by T cell subsets in our tonsil lymphocyte cultures and demonstrate that the magnitude and distribution of IL-21 secretion varies considerably based on tonsil donor, but is not significantly modulated by KSHV infection. Interestingly, RoRγT+ T cells (both CD4+ and CD8+)

contributed substantially to IL-21 secretion and were positively correlated with KSHV infection of plasma cells at 3 dpi. Moreover, IL-21 secretion by CD8+ central memory T cells was positively correlated with both overall KSHV infection and plasma cell targeting.

These results identify IL-21 signaling as a factor that influences the establishment of KSHV infection in B lymphocytes and, together with our previous work, underscores the importance of plasma cell biology in the initial establishment of KSHV infection in the oral lymphoid tissues. Based upon this work, we conclude that specific IL-21 secreting T cell subsets represent an important susceptibility factor for KSHV transmission.

Results

Host cytokines influence the establishment of KSHV infection B lymphocytes

Despite the critical interplay between KSHV and host cytokine signaling, little is known about whether cytokines influence host susceptibility to KSHV infection. In fact, the roles of proinflammatory cytokines during KSHV infection have been studied mostly in naturally-infected human B cell lines derived from PEL [23, 24]. In order to examine whether cytokines alter the early stages of KSHV infection in the tonsil, we quantitated the levels of 13 cytokines in the supernatants of Mock and KSHV-infected tonsil lymphocyte cultures at 3 days post-infection using a bead-based multiplex immunoassay. This dataset includes 33 independent infections using 24 unique tonsil specimens. IL-6, IFNg, TNFa and IL-22 were the most prevalent cytokines in our cultures based on the median values overall (Fig 1A, panel order). IL-6 was the only cytokine significantly induced in KSHV-infected cultures compared to Mock cultures (Fig 1A) and the magnitude of IL-6 induction by KSHV infection is far greater than the effect of infection on any

other cytokine (Fig 1B). This result is consistent with our previous results in cultures containing only naïve B lymphocytes [25]. Our data also reveals statistically significant reductions in IL-5 and IL-4 concentrations in KSHV-infected cultures compared to Mock cultures (Fig 1A), but these changes are very small compared to those seen with IL-6 (Fig 1B). Interestingly, IFNg concentrations were highly affected by KSHV infection, but there were sample-specific differences in whether this effect was positive or negative (Fig 1B).

In order to determine whether cytokines affect the establishment of KSHV infection, we examined whether the concentration of cytokines in the supernatants of KSHV-infected cultures is correlated with the level of infection in B lymphocytes (based on GFP reporter expression) in the same culture by flow cytometry analysis (Fig 1C & D). On a per-sample level, many individual cytokines (notably IL-6 and IFNg) were induced or repressed independent of susceptibility. However, there is a cluster of highly susceptible samples (ND19, ND40, ND41, ND32, ND4) in which multiple cytokines are repressed in the KSHV-infected cultures (Fig 1C). Pairwise comparisons between overall GFP level in B lymphocytes and the level of each cytokine in the KSHV-infected cultures revealed universally negative correlations between overall KSHV infection and cytokine levels with lower cytokine levels observed in more susceptible samples. These negative correlations were statistically significant for IL-2, IL-9, IL-10, TNFa, IL-4 and IL-22 (Fig 1D). Since plasma cells were identified as a highly targeted cell type in our previous study [12], we examined the correlations between cytokine levels in KSHV-infected cultures and infection in the CD138+ plasma cell subset. This analysis revealed negative correlations similar to those seen with overall infection with IL-13, IL-9, IFNg, TNFa and IL-22 levels showing statistically significant negative correlations with plasma cell infection. However, in this analysis IL-21 levels showed a significant positive correlation with plasma cell infection (Fig 1E). Taken together, these data

demonstrate that (1) KSHV infection influences the production of multiple cytokines in our *ex vivo* infection model, (2) lower cytokine levels and/or repression of cytokines during infection are generally associated with higher susceptibility to KSHV infection, (3) several individual cytokines show significant negative associations with susceptibility to KSHV infection and (4) IL-21 is positively correlated with KSHV infection of plasma cells. Overall, these data suggest that distinct inflammatory responses in each tonsil specimen contribute to variable susceptibility to KSHV infection.

IL-21 supplementation increases KSHV infection in tonsil B lymphocytes

Because IL-21 production was positively correlated with plasma cell infection in our initial dataset (Fig 1E), we wanted to examine the impact of manipulating IL-21 levels on the establishment of KSHV infection. To do this, we performed Mock infection or KSHV infection in 12 unique tonsil samples and supplemented the resulting cultures with varying concentrations of recombinant IL-21. At 3 dpi, we analyzed these cultures for GFP+ B lymphocytes by flow cytometry to assess the magnitude of KSHV infection (Fig 2A & B). Although the specimens included in this data set had high variability in their baseline susceptibility, we can see increased infection in response to IL-21 treatment, and the effect seems to be particularly strong in the more susceptible samples (Fig 2A). Normalization of the data to each specimen's untreated control reveals that at 10/12 samples show increased infection upon treatment with 100pg/ml of IL-21. Importantly, most of these concentrations were higher than what was observed in our initial dataset quantitating native cytokine secretion in our culture system (Fig 1A), which may explain why we didn't observe an association of IL-21 secretion with overall infection in that data (Fig 1D). We then repeated these supplementation experiments with only the 100pg/ml dose of recombinant IL-21 in an additional

12 tonsil specimens and examined both overall infection and subset-specific responses in these cultures at 3 dpi using our B cell immunophenotyping panel. Similar to the initial dataset, this analysis shows increased infection in response to recombinant IL-21 in the majority of tonsils, and the difference in GFP+ B lymphocytes was statistically significant in IL-21 treatment compared to control (p=0.02, F=6.4) (Fig 2C).

IL-21 increases plasma cell frequency and susceptibility in primary human tonsil B lymphocytes

In order to determine whether IL-21 signaling influences the overall distribution of B cell subsets in both Mock and KSHV infected cultures, we performed B cell immunophenotyping. Analysis of overall subset frequencies, with all subsets represented as a fraction of viable CD19+ B cells, at 3 dpi revealed that most subsets did not change with either KSHV infection or IL-21 treatment. We did observe a statistically significant increase in CD20+ B cells and plasmablasts in the KSHV-infected conditions independent of IL-21 treatment. Naïve B cells showed significant main effects for both infection and treatment, with both KSHV infection and IL-21 treatment reducing naïve B cells in the culture, but the interaction was not significant. Importantly, this analysis revealed a highly significant increase in total plasma cell frequency associated with both IL-21 treatment and KSHV infection with a significant interaction of the two variables. This effect seems to be restricted to CD20+ plasma cells in the mock conditions and distributed between both CD20+ and CD20- plasma cells in the KSHV-infected cultures. However, both CD20+ and CD20- plasma cells showed statistically significant interactions between infection and treatment (Fig 2D, Table 1). Post hoc paired T tests revealed significant differences with IL-21 treatment on total plasma cells (p=0.0002) and CD20+ plasma cells (p=0.002) for the KSHV-infected conditions only. The

IL-21 effect on naïve B cell frequencies was significant for both Mock (p=0.01) and KSHV infected conditions (p=0.003). Moreover, in IL-21 treated conditions there was a significant difference between Mock and KSHV cultures for total plasma cells (p=0.0003), CD20+ plasma cells (p=0.02) and naïve B cells (p=0.006). One interpretation of this data is that IL-21 can independently drive plasma cell differentiation of B cells in our culture system resulting in decreased naïve cells and increased plasmablast and plasma cells, and KSHV infection acts synergistically with IL-21 to potentiate the same effect. We next wanted to determine whether IL-21 treatment altered the B cell subset-specific distribution of KSHV infection. For this analysis, we quantitated the percent of each B cell subset that was GFP+ to determine the within-subsets distribution of KSHV infection in control or IL-21 treated cultures (Fig 2E). In this analysis, we observed a significant increase in plasma cell targeting with IL-21 treatment (p=0.02, F=6.6). We next examined whether increased frequency of plasma cells or increased plasma cell targeting was directly correlated with the observed increase in overall KSHV infection in the IL-21 treated conditions (Fig 2F). These results reveal a significant linear correlation between total GFP and plasma cell frequency (r=0.7, p=0.007) and a weaker correlation between total GFP and the frequency of GFP+ cells within the plasma cell subset (r=0.56, p=0.04).

Taken together this data shows that IL-21 treatment promotes the establishment of KSHV infection in human tonsil lymphocytes and that this increased infection is correlated with both increased plasma cell frequencies and increased plasma cell infection. Thus, our results suggest that IL-21 signaling facilitates the establishment of KSHV infection by driving the proliferation, survival or differentiation of plasma cells in our tonsil lymphocyte cultures. The observation that naïve B cell frequencies are significantly decreased in KSHV-infected, IL-21-treated cultures (Fig 2D)

supports the latter conclusion that increased plasma cell frequencies are a result of B cell differentiation in response to IL-21 signaling.

Table 1: Statistically significant effects from two-way repeated measures ANOVA analysis in Fig 2D

Variable	Effect	DFn	DFd	F	p	ges
GFP	Treatment	1	13	6.425	0.025	0.081
GFP	Infection	1	13	102.896	1.52e-07	0.708
GFP	Tx:Inf	1	13	7.635	0.016	0.084
Plasma cells	Treatment	1	13	18.596	0.000844	0.163
Plasma cells	Infection	1	13	18.575	0.000848	0.166
Plasma cells (PC)	Tx:Inf	1	13	22.779	0.000364	0.09
Naive	Treatment	1	13	13.643	0.003	0.099
Naive	Infection	1	13	8.462	0.012	0.069
Plasmablast	Infection	1	13	6.023	0.029	0.02
CD20- PC	Tx:Inf	1	13	12.645	0.004	0.043
All CD20+CD19+	Infection	1	13	6.234	0.027	0.016
CD20+ PC	Treatment	1	13	4.858	0.046	0.028
CD20+ PC	Tx:Inf	1	13	7.798	0.015	0.012

<u>Neutralization of IL-21 inhibits KSHV infection in primary tonsil B lymphocytes</u>

We next wanted to determine whether neutralization of the natively-secreted IL-21 in our tonsil lymphocyte cultures would affect the establishment of KSHV infection. To do this we performed infections with Mock or KSHV-infection in 11 unique tonsil specimens, included varying concentrations of an IL-21 neutralizing antibody in the resulting cultures, and assessed the magnitude and distribution of KSHV infection at 3 dpi by flow cytometry. These results revealed decreased KSHV infection in the presence of IL-21 neutralizing antibodies (Fig 3A). One-way repeated measures ANOVA revealed a significant effect of IL-21 neutralization on GFP in KSHV infected cultures ($p=0.00001$, $F=9.4$) and post-hoc Dunnett test revealed significance at the 100µg/ml dose ($p=0.03$). When each sample was normalized to its untreated control, we observed that 9/11 samples had decreased infection in the presence of 100µg/ml IL-21 neutralizing antibody and this increased to 10/11 samples at higher antibody doses (Fig 3B).

When we examined the overall frequency of B cell subsets at 3dpi in these experiments, we observed statistically significant effects of IL-21 neutralization on a number of B cell subsets, but there were no significant interaction effects with IL-21 neutralization and KSHV infection using two-way repeated measures ANOVA (Fig 3C). Specifically, IL-21 neutralization increased IgG+ ($p=0.04$, $F=5.0$), memory ($p=0.03$, $F=3.4$), and double negative ($p=0.02$, $F=3.8$) B cells and decreased IgM+ ($p=0.0003$, $F=8.6$) and transitional ($p=0.01$, $F=4.1$) subsets. Post-hoc paired T-tests showed a statistically significant decrease of on both overall ($p=0.02$) and CD20+ ($p=0.005$) plasma cell frequencies at the 200µg/ml dose in the mock infected cultures only. The observation that the effect of IL-21 neutralization on plasma cell frequencies is restricted to mock infected cultures is interesting in the context of our IL-21 supplementation data where we observed significant main effects of both IL-21 and KSHV infection on plasma cell frequencies as well as a significant interaction between the two factors (Fig 2D & Table 1). The two data sets taken together

support several interesting conclusions: (1) IL-21 affects plasma cell frequencies independent of KSHV infection; evidenced by opposite significant effects of IL-21 supplementation and neutralization in mock cultures, (2) KSHV infection affects plasma cell frequencies independent of IL-21 signaling; evidenced by significant main effect of infection in supplemented cultures and a lack of inhibition in KSHV-infected neutralized cultures, and (3) IL-21 and KSHV can synergistically affect plasma cell frequencies; evidenced by the significant interaction effect and the significant increase in plasma cell frequencies in KSHV-infected cultures that are supplemented with IL-21.

We next wanted to determine whether neutralization of IL-21 influences the frequency of KSHV infection within B cell subsets. One-way repeated measures ANOVA revealed a significant effect of neutralization on infection of transitional B cells ($p=0.01$, $F=4.0$) but paired T tests were not significant for any individual dose. When we plotted this data normalized to the per-sample, per-subset infection rate of the untreated control cultures, we observed that neutralization was associated with lower levels of infection in transitional, plasmablast, and CD20+ PC populations (Fig 3D). We hypothesized that if IL-21 signaling is affecting overall infection by contributing substantially to differentiation of KSHV-infected cells, we might observe a correlation between overall infection and the contribution of specific subsets to infection within neutralized cultures compared to control cultures. If this hypothesis is correct, subsets whose differentiation is important to the establishment of infection would accumulate with IL-21 neutralization and this accumulation would correlate with decreased overall levels of infection in the same cultures. To examine this, we calculated the change in IL-21 neutralized cultures compared to control cultures (neutralized-control) for both overall infection and the contribution of each subset to infection (between subsets frequency of GFP), and performed correlation analysis using Pearson’s method.

This analysis reveals that decreased overall infection with IL-21 neutralization was significantly correlated with a decreased contribution of plasma cells (r=0.6, p=0.0002), CD20+ plasma cells (r=0.6, p=0.0002), and transitional B cells (r=0.5, p=0.003) and an increased proportion of infected germinal center cells (r=-0.4, p=0.02) (Fig 3E). Interestingly, these correlations were driven more by sample-specific differences (indicated by point color) compared to dose response of neutralization (indicated by point shape). This data could indicate that IL-21 signaling increases the overall establishment of KSHV infection in tonsil lymphocytes by driving differentiation of KSHV-infected germinal center cells into transitional and CD20+ plasma cells. Our previous studies demonstrated that plasma cells display a mixture of lytic and latent KSHV infection [12]. Therefore, we wanted to determine whether the increase in overall KSHV infection with IL-21 treatment and decrease in infection with IL-21 neutralization is due to IL-21-mediated alterations in KSHV lytic reactivation. To examine this, we performed RT-PCR for LANA (latent) and K8.1 (lytic) on total RNA from untreated, IL-21 supplemented or IL-21 neutralizing antibody treated, KSHV-infected cultures from 8 unique tonsil specimens. GAPDH was used as a housekeeping gene and normalizing factor for the viral gene expression data. This data is consistent with our previous data showing a mix of lytic and latent transcripts in infected lymphocytes [12]. These data reveal no significant influence of either supplementation or neutralization on lytic gene expression (Fig 3F). In the majority of samples K8.1 expression remained unchanged or changes were also reflected in LANA transcripts (Fig 3G).

IL21 receptor distribution in primary human tonsil B lymphocytes affects the magnitude and distribution of KSHV infection

Our data presented thus far demonstrates that IL-21 signaling has a positive effect on the overall establishment of KSHV infection (Fig 2C and 3B) and this increase in overall infection is related to both the absolute number of plasma cells (Fig 2D&F and 3C), and the establishment of infection in plasma cells (Fig 2E&F and 3E). Moreover, our data suggests that the increase in plasma cell numbers and targeting may be due to differentiation of new plasma cells via a process that requires IL-21 signaling to germinal center B cells (Fig 3E). To further address the early stages of the IL-21 response during infection, we examined expression of the IL21 receptor in primary human tonsil B lymphocytes at baseline (day 0) in each tonsil specimen. We observed that IL-21 receptor expression is rare on B cells in tonsil at less than 3% of total viable B cells in most samples (Fig 4A). The distribution of IL-21 receptor positive cells among B cell sub-populations is broad, but IL-21 receptor-expressing B cells are most likely to have an MZ-like or plasmablast immunophenotype (Fig 4B) and on a per-sample basis, either plasmablast or MZ-like subsets dominated the IL-21R positive cells in most tonsil samples (Fig 4C)

In order to determine whether IL-21 receptor expression at baseline influenced the establishment of KSHV infection, we aggregated the untreated conditions from both the supplementation and the neutralization experiments and examined correlations between baseline IL21R distribution and KSHV infection based on overall GFP. This analysis revealed that the proportion of plasmablasts within IL21R+ B cells is significantly correlated with overall susceptibility to KSHV infection ($r=0.81$, $p=0.0007$) (Fig 4D). In experiments where we supplemented cultures with IL-21, the positive effect of IL-21 treatment on overall KSHV infection at 3 dpi (Fig 2C) is correlated with the baseline frequency of IL-21 receptor expression on naïve B cells ($r=0.82$, $p=0.01$) and classical memory B cells ($r=0.7$, $p=0.05$) (Fig 4E). The significant correlation between the IL-21 response and baseline IL-21 receptor expression is particularly interesting and consistent with our

hypothesis that differentiation of naïve B cells into plasma cells contributes to the increase in overall infection we see with IL-21 treatment (Fig 2D).

When we correlated baseline IL21R expression with the positive effect of IL-21 treatment on total plasma cell numbers in KSHV-infected cultures (Fig 2D), no significant positive correlations were found (Fig 4F). This lack of correlation suggests that the plasma cell response to IL-21 at 3 dpi in KSHV infected cultures may be a product of IL-21 receptor up-regulation in response to infection instead of intrinsic baseline levels of IL-21 on plasma cells or plasma cell precursors in our tonsil lymphocyte cultures. Indeed, modulation of IL-21 receptor expression by KSHV infection could be one mechanism for the synergistic promotion of plasma cell numbers we observe with both IL-21 treatment and infection (Fig 2D).

In order to examine this hypothesis, we analyzed IL-21R expression on B cell subsets at 3 dpi in our culture system with or without IL-21 supplementation to determine whether KSHV and/or IL-21 can modulate the response to IL-21 during infection. These results reveal that the majority of effects on IL-21R at 3 dpi are present in both Mock and KSHV-infected cultures, indicating they are a product of the culture system and not driven by KSHV. However, the proportion of plasmablasts within IL21R+ cells was significantly different comparing Mock to KSHV-infected cultures without IL-21 treatment ($p=0.03$) and this difference was increased with the combination of KSHV infection and IL-21 treatment (Fig 4G). This result may indicate that infection is affecting IL21R expression on plasmablasts or that KSHV is infecting a precursor B cell and driving differentiation of these cells into IL21R+ plasmablasts. Taken together with the fact that IL-21R expression on plasmablasts at day 0 is highly correlated with overall infection (Fig 4D), these data strongly suggest that plasmablasts play a role in the response of KSHV infection to IL-

21 treatment. Although not statistically significant, a similar trend can be observed for IL21R+ plasma cells while the converse trend is seen for IL21R positive germinal center cells (Fig 4G), these observations are consistent with the data from our IL21 neutralization studies that suggests germinal center cells may be differentiating into plasma cells in response to IL-21 signaling (Fig 3E), potentially via a plasmablast intermediate phenotype.

Characterization of T cell subsets producing IL-21 in primary human tonsil B lymphocytes

We next wanted to determine the source of native IL-21 secretion in our culture system, and determine whether the production of IL-21 is affected by KSHV infection. To accomplish this, we utilized an additional immunophenotyping panel for T cell subsets (Table 2 and Supplemental Fig 1) and performed intracellular cytokine staining (ICCS) to identify IL-21 producing T cells at 3 dpi in Mock and KHSV-infected cultures from 14 unique tonsil samples. This data reveals that IL-21 secretion in T cells is highly variable between tonsil lymphocyte cultures, but is not significantly affected by KSHV infection (Fig 5A). More of the IL-21+ cells were CD4+ T cells vs. CD8+ T cells and this distribution was also not affected by KSHV infection (Fig 5B). When we examined the subset-level distribution of IL-21 secretion within T cells, we observed that within CD4+ cells CD45RO+, central memory, TFH and RoRγT+ cells were contributing most to IL-21 secretion. Among CD8+ T cells, CD45RA+, stem cell memory, central memory and RoRγT+ cells were the highest contributors to IL-21 secretion (Fig 5C). When we examined whether KSHV infection altered the contribution of T cell subsets to IL-21 secretion in these cultures, we found that the contribution of CD4+ CD45RA+, CD4+ RoRγT+ and CD8+ central memory subsets was significantly decreased in KSHV-infected cultures vs. Mock cultures (Fig 5D). However, KSHV infection did not significantly change the overall levels and subset distribution of T cells within

these cultures, indicating these are biological changes within T cell subsets and not due to changes in the T cell population during infection (Supplemental Fig 2).

Table 2: Lineage definitions for lymphocyte subsets used in the study	
B Lymphocytes	
Subset	**Molecular Markers**
Plasma	$CD19^{+}$, $CD20^{+/-}$, $CD138^{+(Mid\ to\ High)}$, $CD38^{-}$
Transitional	$CD19^{+}$, $CD138^{-}$, $CD38^{Mid}$, $IgD^{+\ (Mid\ to\ High)}$
Plasmablast	$CD19^{+}$, $CD138^{-}$, $CD38^{High}$, $IgD^{+\ /-\ (mostly\ -)}$
Germinal Center	$CD19^{+}$, $CD138^{-}$, $CD38^{Mid}$, IgD^{-}
Naïve	$CD19^{+}$, $CD138^{-}$, $CD38^{Low}$, $CD27^{-}$, $IgD^{+\ (Mid\ to\ High)}$
Marginal Zone Like (MZ-Like)	$CD19^{+}$, $CD138^{-}$, $CD38^{Low}$, $CD27^{+\ (Mid\ to\ High)}$, $IgD^{+\ (Mid\ to\ High)}$
Memory	$CD19^{+}$, $CD138^{-}$, $CD38^{Low}$, $CD27^{+\ (Mid\ to\ High)}$, IgD^{-}
Double Negative	$CD19^{+}$, $CD138^{-}$, $CD38^{Low}$, $CD27^{-}$, IgD^{-}
T lymphocytes	
Subset	**Molecular Markers**
CD4+	$CD19^{-}$, $CD4^{+(Mid\ to\ High)}$, $CD8^{-}$
CD8+	$CD19^{-}$, $CD4^{-}$, $CD8^{+\ (Mid\ to\ High)}$
Naïve	$CD19^{-}$, CD4+ or CD8+, $CCR7^{+(High)}$, $CD45RA^{+(Mid\ to\ High)}$, $CD45RO^{-}$, $CD28^{+}$, $CD95^{-}$
Stem Cell Memory	$CD19^{-}$, CD4+ or CD8+, $CCR7^{+(High)}$, $CD45RA^{+(Mid\ to\ High)}$, $CD45RO^{-}$, $CD28^{+}$, $CD95^{+\ (Low\ to\ Mid)}$
Central Memory	$CD19^{-}$, CD4+ or CD8+, $CCR7^{+}$, $CD45RA^{-}$ $CD45RO^{+(Mid\ to\ High)}$, $CD28^{+\ (Mid\ to\ High)}$
Transitional Memory	$CD19^{-}$, CD4+ or CD8+, $CCR7^{-}$, $CD45RA^{-}$ $CD45RO^{+(Mid)}$, $CD28^{+\ (Mid\ to\ High)}$
Effector Memory	$CD19^{-}$, CD4+ or CD8+, $CCR7^{-}$, $CD45RA^{-}$ $CD45RO^{+(Mid)}$, $CD28^{-}$
Terminal Effector Memory	$CD19^{-}$, CD4+ or CD8+, $CCR7^{-}$, $CD45RA^{-}$ $CD45RO^{-}$, $CD28^{-}$
TEMRA CD4+ Cells	$CD19^{-}$, CD4+ or CD8+, $CCR7^{-}$, $CD45RA^{+(High)}$, $CD45RO^{-}$, $CD28^{-}$
Tfh	CD19-, CD4+, CD8- , PD-1+, CXCR5+, CD127+, Intracellular BCL-6+
Treg	CD19-, CD4+, CD8- , CD25+, CD127+, Intracellular FoxP3+
Th17	CD19-, CD4+, CD8- , Intracellular ROR gamma T+

IL-21 secretion by CD8+ central memory T cells influences both overall KSHV infection and plasma cell targeting

We wanted to determine whether IL-21 secretion by any particular T cell subset was correlated with susceptibility to KSHV infection in our experiments. To do this, we performed B cell immunophenotyping analysis to determine the extent and distribution of KSHV infection in the same cultures where ICCS was performed on T cell subsets. When we examined correlations between IL-21 secretion by T cell subsets and overall KSHV infection in B cells we found that only IL-21+ CD8+ central memory cells were significantly correlated ($r=0.57$, $p=0.03$) (Fig 6A). Interestingly, when we examined correlations between IL-21+ T cell subsets and the B cell subset-specific distribution of KSHV infection at 3dpi, we found that the positive correlation between IL-21+ CD8+ central memory T cells is coupled with a highly significant positive correlation to the targeting of plasma cells ($r=0.82$, $p=0.0003$) (Fig 6B & 6C). In addition, both CD4+ and CD8+ IL-21+ T cells that express RoRγT+ (the Th17/Tc17-defining transcription factor) were significantly correlated with plasma cell targeting by KSHV (Fig 6B & 6D). These correlations were stronger for CD4+ cells and were coupled with a negative correlation with KSHV-infection of naïve T cells (Fig 6B). When we examined whether baseline (day 0) frequencies of T cell subsets influenced the magnitude and distribution of KSHV infection at 3dpi we found several interesting correlations (1) frequencies of CD8+ central memory cells significantly correlated with KSHV targeting of plasma cell subsets (Fig 6E and 6F), (2) baseline frequencies of CD4+ RoRγT+ cells significantly correlated with infection of CD20+ plasma cells (Fig 6D) and (3) both CD4+ and CD8+ RoRγT+ were negatively correlated with KSHV infection of naïve B cells at 3dpi (Fig 6D). Taken together, these results support a hypothetical model in which CD8+ central memory T cells secrete IL-21, which supports the differentiation, survival or targeting of plasma cells, resulting in

higher plasma cell infection frequencies and also an overall increase in dissemination of KSHV within B lymphocytes. Our data also support the conclusion that RoRγT+ T cells are participating in KSHV targeting of plasma cells via IL-21 signaling, possibly by mediating differentiation of naïve B cells, but this effect does not have a significant influence on overall infection in this data set.

Discussion

Our results presented in this study indicate that KSHV can influence cytokine production in tonsil-derived lymphocytes and that the host inflammatory state contributes to the dramatic variation in susceptibility we observe among our tonsil lymphocyte specimens [12]. This result is not surprising considering dysregulation of the inflammatory environment is a hallmark of all KSHV-associated malignancies [24, 26, 27]. However, the role of the baseline inflammatory environment in the oral cavity as a potentially modifiable susceptibility factor for the acquisition of KSHV infection in humans is an interesting consideration stemming from these results that deserves further study.

Our previous work demonstrated that plasma cells are highly targeted during early KSHV infection, and subsequent results from our group have shown that manipulations which increase plasma cell numbers also increase overall KSHV infection in B cells [28]. This latter observation suggested that, in addition to being a highly targeted cell type, plasma cells are playing an active role in early infection events that ultimately influences the success of initial dissemination for KSHV within the B cell compartment. The results presented herein are consistent with that conclusion, and mechanistically extend our understanding of how the immune microenvironment

influences the establishment of infection in plasma cells. Specifically, we uncovered a critical role for IL-21 signaling in this process.

While the precise role of IL-21 and IL-21R in human KSHV disease is poorly characterized, IL-21 has been studied in the pathogenesis of chronic lymphocytic choriomeningitis virus (LCMV) infection, influenza virus, and, perhaps most relevant to this study, murine gammaherpesvirus 68 (MHV68) [22, 29, 30]. Collins and Speck recently used IL-21R knockout mice to demonstrate that IL-21 signaling is critical for the establishment of MHV68 latency specifically in B cells. Interestingly, this study showed that the mechanisms of decreased infection were related to decreases in both germinal center and plasma cell frequencies as well as decreased infection in both the germinal center and plasma cell compartment at later timepoints post-infection [22], suggesting a critical mechanism for IL-21 in MHV68 transit of the germinal center and differentiation of follicular-derived plasma cells. These results are generally consistent with our current findings showing that IL-21 signaling promotes KSHV infection and dissemination in tonsil via promotion of both plasma cell frequencies and plasma cell targeting (Fig 2&3), potentially via differentiation through a germinal center intermediate (Fig 3E). Despite this, our data presented herein do not adequately address the question of whether plasma cells are differentiating in response to KSHV infection and IL-21 signaling, or whether the effect we see is increased survival or expansion of existing plasma cells. Studies are currently ongoing to address this question more directly, and to examine the influence of viral and cellular factors on B cell differentiation in our model system.

Moreover, both IL-21 and IL-6, which is highly induced in our KSHV-infected cultures (Fig 1), are involved in the generation of RoRγT+ T cells via STAT3 signaling. The resulting Th17 cells

produce IL-17A which is another cytokine that promotes the establishment of chronic MHV68 infection via promotion of the MHV68-mediated germinal center response [31] and is mechanistically linked to suppression of T cell-intrinsic IRF-1 [32]. These results are particularly interesting in light of our current findings showing that IL-21 secretion from, and baseline levels of, RoRγT+ T cells correlate with the early targeting of plasma cells during KSHV infection (Fig 6B and 6D), suggesting that the Th17/Tc17 environment in the tonsil may be a critical factor influencing donor-specific susceptibility to KSHV infection. Indeed, as an important site for mucosal immunity in the oral cavity, the Th17/Tc17 environment in tonsil is highly dynamic and physiologically important. In fact, Th17 cells play a major role in host defenses against several pathogens and immunopathogenesis [33, 34]. Many studies have shown that certain parasites modulate the immune response by inducing Th17 [35, 36]. Previous finding suggest that parasite infection is linked with KSHV infection in Uganda [37]. Thus, the parasite burden in sub-Saharan Africa may modulate susceptibility to KSHV infection via manipulating Th17/Tc17 frequencies.

Consistent with the MHV68 literature, our current results mechanistically implicate germinal center cells in these observations. However, although our *ex vivo* model of KSHV infection in primary lymphocytes is a powerful tool, it certainly does not recapitulate the complex interactions that are needed for a functional germinal center reaction, so further examination of these particular mechanisms will require the utilization of an alternative model system, such as a humanized mouse. Interestingly, neither IL-21 secretion from, nor baseline levels of, CXCR5+, PD1+ TFH cells correlated with increased KSHV infection or increased plasma cell targeting in our study. This was surprising given that TFH are generally considered the canonical IL-21 producing cells in secondary lymphoid organs [38]. This observation may indicate that IL-21 acts support plasma

cell numbers during infection via an extrafollicular pathway, which is consistent with literature implicating extrafollicular maturation of KSHV-infected B cells in the pathogenesis of MCD [39].

We observed that IL-21 secretion by CD8+ T cells with a central memory immunophenotype (CCR7+CD45RO+CD28+) was significantly correlated with both overall KSHV infection and plasma cell targeting, and baseline levels of CD8+ central memory T cells were also correlated with plasma cell targeting at 3 dpi (Fig 6). Interestingly, recent studies have shown that IL-6 regulates IL-21 production in CD8+ T cells in a STAT3-dependent manner, and that CD8+ T cells induced in this way can effectively provide help to B cells [40]. Thus, the induction of human IL-6 during KSHV infection may modulate the function of CD8+ T cells in a way that favors the establishment and dissemination of KSHV infection within the lymphocyte compartment independent of traditional CD4+ helper T cells, which would be an interesting dynamic in the context of CD4+ T cell immunosuppression associated with HIV infection where KSHV-mediated malignancies are common.

Material and Methods

Ethics Statement. Human specimens used in this research were de-identified prior to receipt, and thus were not subject to IRB review as human subjects research.

Reagents and Cell Lines. CDw32 L cells (CRL-10680) were obtained from ATCC and were cultured in DMEM supplemented with 20% FBS (Sigma Aldrich) and Penicililin/Streptomycin/L-glutamine (PSG/Corning). For preparation of feeder cells CDw32 L cells were trypsinized and resuspended in 15 ml of media in a petri dish and irradiated with 45 Gy of X-ray radiation using a Rad-Source (RS200) irradiator. Irradiated cells were then counted and cyropreserved until needed

for experiments. Cell-free KSHV.219 virus derived from iSLK cells [39] was a gift from Javier G. Ogembo (City of Hope). Human tonsil specimens were obtained from the National Disease Research Interchange (NDRI; ndriresource.org). Human fibroblasts for viral titering were derived from primary human tonsil tissue and immortalized using HPV E6/E7 lentivirus derived from PA317 LXSN 16E6E7 cells (ATCC CRL-2203). Antibodies for flow cytometry were from BD Biosciences and Biolegend and are detailed below. Recombinant human IL-21 was from Preprotech (200-21) and IL-21 neutralizing antibody was from R&D Systems (991-R2).

***Isolation of primary lymphocytes from human tonsils*.** De-identified human tonsil specimens were obtained after routine tonsillectomy by NDRI and shipped overnight on wet ice in DMEM+PSG. All specimens were received in the laboratory less than 24 hours post-surgery and were kept at 4˚C throughout the collection and transportation process. Lymphocytes were extracted by dissection and maceration of the tissue in RPMI media. Lymphocyte-containing media was passed through a 40µm filter and pelleted at 1500rpm for 5 minutes. RBC were lysed for 5 minutes in sterile RBC lysing solution (0.15M ammonium chloride, 10mM potassium bicarbonate, 0.1M EDTA). After dilution to 50ml with PBS, lymphocytes were counted, and pelleted. Aliquots of 5(10)7 to 1(10)8 cells were resuspended in 1ml of freezing media containing 90% FBS and 10% DMSO and cryopreserved until needed for experiments.

***Infection of primary lymphocytes with KSHV*.** Lymphocytes were thawed rapidly at 37˚C, diluted dropwise to 5ml with RPMI and pelleted. Pellets were resuspended in 1ml RPMI+20%FBS+100µg/ml DNaseI+ Primocin 100µg/ml and allowed to recover in a low-binding 24 well plate for 2 hours at 37˚C, 5% CO2. After recovery, total lymphocytes were counted and naïve B cells were isolated using Mojosort Naïve B cell isolation beads (Biolegend 480068) or Naïve B cell Isolation Kit II (Miltenyi 130-091-150) according to manufacturer instructions.

Bound cells (non-naïve B and other lymphocytes) were retained and kept at 37˚C in RPMI+20% FBS+ Primocin 100µg/ml during the initial infection process. 1(10)[6] Isolated naïve B cells were infected with iSLK-derived KSHV.219 (dose equivalent to the ID20 at 3dpi on human fibroblasts) or Mock infected in 400ul of total of virus + serum free RPMI in 12x75mm round bottom tubes via spinoculation at 1000rpm for 30 minutes at 4˚C followed by incubation at 37˚C for an additional 30 minutes. Following infection, cells were plated on irradiated CDW32 feeder cells in a 48 well plate, reserved bound cell fractions were added back to the infected cell cultures, and FBS and Primocin (Invivogen) were added to final concentrations of 20% and 100µg/ml, respectively and recombinant cytokines or neutralizing antibodies were also added at this stage, depending upon the specific experiment. Cultures were incubated at 37˚C, 5% CO2 for the duration of the experiment. At 3 days post-infection, cells were harvested for analysis by flow cytometry and supernatants were harvested, clarified by centrifugation for 15 minutes at 15,000 rpm to remove cellular debris, and stored at -80˚C for analysis.

***Bead-based immunoassay for supernatant cytokines*.** Clarified supernatants were thawed on ice and 25µl of each was added to a 13-plex LEGENDplex (Biolegend) bead-based immunoassay containing capture beads for the following analytes: IL-5, IL-13, IL-2, IL-9, IL-10, IL17A, IL-17F, IL-6, IL-21, IL-22, IL-4, TNF-α, and IFN-γ. These assays were performed according to the manufacturer's instructions, data was acquired for 5000 beads per sample (based on approximately 300 beads per analyte recommended by the manufacturer) using a BD FACS VERSE flow cytometry analyzer and cytokine concentrations in the experimental supernatants was calculated from standard curves using the LEGENDPlex software.

Flow cytometry analysis of baseline lymphocyte subsets and KSHV infection. Approximately 5(10)^6 lymphocytes per condition were harvested into a 96- well round bottom plate at day 0 (baseline) or at 3 days post-infection at 1500 rpm for 5 minutes. Cells were resuspended in 100µl PBS containing zombie violet fixable viability stain (BL Cat# 423113) and incubated on ice for 15 minutes. After incubation, cells were pelleted and resuspended in 100ul PBS, containing the following: 2% FBS and 0.5% BSA (FACS Block) was added to the wells. Cells were pelleted at 1500rpm 5 minutes and resuspended in 200ul FACS Block for 10 minutes on ice. Cells were pelleted at 1500rpm for 5 minutes and resuspended in 50µl of PBS with 0.5% BSA and 0.1% Sodium Azide (FACS Wash), **For B cell frequencies** 10µl BD Brilliant Stain Buffer Plus and antibodies as follows: IgD-BUV395 (2.5µl/test BD 563823), CD77-BV510 (2.0 µl/ test BD 563630), CD138- BV650 (2µl/test BD 555462), CD27-BV750 (2µ/test BD 563328), CD19-PerCPCy5.5 (2.0µl/test BD 561295), CD38-APC (10µl/test BD 560158), CD20-APCH7 (2ul/test BL 302313), IgM (2µl/test BL 314524), IgG (2µl/test BD 561298), IgE (2µl/test BD 744319) and IL-21 receptor (2µl/test BD 330114). **For baseline T cell frequencies**. For baseline T cell frequencies 0.5(10)^6 cells from baseline uninfected total lymphocyte samples were stained and analyzed as above with phenotype antibody panel as follows: CD95-APC (2µl, Biolegend 305611), CCR7-PE (2µl, BD 566742), CD28-PE Cy7 (2µl, Biolegend 302925), CD45RO-FITC (3µl, Biolegend 304204), CD45RA-PerCP Cy5.5 (2µl, 304121), CD4-APC H7 (2µl, BD 560158), CD19-V510 (3µl, BD 562953), CD8-V450 (2.5µl, BD 561426). and incubated on ice for 15 minutes. After incubation, 150µl FACS Wash was added. Cells were pelleted at 1500rpm for 5 minutes followed by two washes with FACS Wash. Cells were collected in 200µl FACS Wash for flow cytometry analysis. Cells were analyzed using an LSR Fortessa X-20 cell analyzer (BD Biosciences). BD CompBeads (51-90-9001229) were used to calculate compensation for all

antibody stains and methanol-fixed Namalwa cells (ATCC CRL1432) +/- KSHV were used to calculate compensation for GFP and the fixable viability stain. Flow cytometry data was analyzed using FlowJo software and exported for quantitative analysis in R as described below.

ICCS for IL-21 secretion. At 3dpi, cultures were treated for 6 hours with [4 ul for every 6ml of cel culture] monensin to block cytokine secretion. Following incubation, approximately 1 million cells were harvested and viability and surface staining for T cell lineage markers was performed as described above. After the final wash, cells were fixed for 10 minutes in BD cytofix/cytoperm (51-2090KZ), pelleted and further treated for 10 minutes with cytofix/cytoperm+10% DMSO (superperm) to more effectively get intracellular antibodies into the nucleus. Intracellular antibodies, as follows, were diluted in 1x BD Permwash (51-2091KZ) and left on fixed cells overnight at 4˚C. RoR-γT-BV421 (563282, 5µl/test), FoxP3-BB700 (566527, 5 µl/test), IL-21-APC (513007, 5 µl/test), BLC6-BV711 (561080, 5µl/test). Cells were then washed twice with 1x permwash and analyzed as described above.

RT-PCR. At 3 days post infection, $1(10)^6$ lymphocytes were harvested into an equal volume of Trizol and DNA/RNA shield (Zymo Research R110-250). Total RNA was extracted using using Zymo Directzol Microprep (Zymo Research R2060) according to manufacturer instructions. RNA was eluted in 10µl H2O containing 2U RNase inhibitors and a second DNase step was performed for 30 minutes using the Turbo DNA-Free kit (Invitrogen AM1907M) according to manufacturer instructions. One-step RT-PCR cDNA synthesis and preamplification of GAPDH, LANA and K8.1 transcripts was performed on 15ng of total RNA using the Superscript III One-step RT-PCR kit (ThermoFisher 12574026).

Duplicate no RT (NRT) control reactions were assembled for each sample containing only Platinum Taq DNA polymerase (Thermofisher 15966005) instead of the Superscript III RT/Taq DNA polymerase mix. After cDNA synthesis and 20 cycles of target pre-amplification, 2µl of pre-amplified cDNA or NRT control reaction was used as template for multiplexed real-time PCR reactions using TaqProbe 5x qPCR MasterMix -Multiplex (ABM MasterMix-5PM), 5% DMSO, primers at 900nM and probes at 250nM against target genes. All primer and probe sequences used in these assays have been previously published [12]. Real time PCR was performed using a 40-cycle program on a Biorad real time thermocycler. Data is represented as quantitation cycle (Cq) and assays in which there was no detectable Cq value were set numerically as Cq = 41 for analysis and data visualization. The expression of each gene was normalized to that of a housekeeping gene *GAPDH*.

Statistical Analysis. The indicated data sets and statistical analysis were performed in Rstudio software using ggplot2 [41], ggcorrplo [42] , and tidyverse [43] packages. Statistical analysis was performed using rstatix [44] package. Specific methods of statistical analysis including Anova, independent t-test and Pearson correlations and resulting values for significance and correlation are detailed in the corresponding figure legends.

Figure Legends

Figure 1: KSHV alters cytokine secretion and cytokines affect the establishment of infection. 33 replicate infections using 24 unique tonsil specimens were performed using KSHV.219 infection of naïve B lymphocytes followed by reconstitution of the total lymphocyte environment and culture on CDW32 feeder cells. At 3 dpi, cells were collected for flow cytometry analysis for

infection (GFP) and B cell subsets using our previously-characterized immunophenotyping panel and supernatants were collected for analysis of cytokines by multiplex immunoassay (Biolegend Legendplex) **(A)** cytokine production in Mock and KSHV-infected cultures showing individual sample quantities and means (red diamonds, top panels) and matched Mock and KSHV samples to show trends of induction/repression (bottom panels) Statistical analysis was performed by one-way repeated measures ANOVA. p=0.01 F=7.06 for IL-5, p=0.0001 F=14 for IL-6, p=0.5 F=4.3 for IL-4 **(B)** Data as in (A) showing the level of induction or repression of each cytokine comparing KSHV to matched Mock cultures **(C)** Induction or repression of all cytokines (left y-axis) on a per-sample basis ordered based on overall susceptibility based on percentage of GFP+ B lymphocytes in the same culture (right y-axis, red diamonds) **(D)** Pairwise correlations using Pearson method between cytokine concentration (y-axis) and overall infection (x-axis) in KSHV-infected lymphocyte cultures **(E)** Pairwise correlations using Pearson method between cytokine concentration (y-axis) and Percent GFP+ within CD138+ (x-axis) in KSHV-infected lymphocyte cultures. For panels A, B, D and E colors indicate individual tonsil specimens and can be compared between panels.

Figure 2: IL-21 supplementation increases overall KSHV infection and plasma cell frequencies. Lymphocytes from 12 tonsil donors were infected with KSHV.219 and cultured with indicated doses of recombinant human IL-21 and analyzed at 3dpi by flow cytometry (A) the dose effect of IL-21 supplementation on GFP+ viable B lymphocytes. (B) data as in (A) normalized to the untreated control for each specimen. (C) 14 additional tonsil donors analyzed as in (A) with only 100pg/ml IL-21 treatment. Red diamonds indicate group means. p=0.02, F=6.4 via one-way repeated measures ANOVA. (D) tonsil lymphocyte specimens from (C) were stained for B cell

immunophenotypes and analyzed by flow cytometry. Red boxes indicate subsets with significant main effects of, and/or interactions between, KSHV infection and IL-21 treatment by two-way repeated measures ANOVA analysis. See Table 1 for p-values and F statistics from this analysis. (E) immunophenotyping data was used to determine the within-subset frequency of GFP+ cells in the KSHV-infected conditions with or without IL-21 treatment. Top panels show individual sample quantities and means (red diamonds) and bottom panels show trends of increased/decreased subset targeting on a per-sample basis. Colored points denote unique tonsil specimens and can be compared between panels D and E. (F) Pearson correlation between overall GFP+ B cells in KSHV-infected, IL-21 treated cultures as in (C) and the level of plasma cells (right) and infection of plasma cells (left). Blue line is linear model regression and grey shading indicates 95% confidence interval.

Figure 3: IL-21 neutralization inhibits the establishment of KSHV infection. Naïve B cells from 11 unique tonsil specimens were Mock or KSHV-infected and indicated concentrations of IL-21 neutralizing antibody was added to the resulting total lymphocyte cultures. Cultures were analyzed at 3 dpi for B lymphocyte immunophenotypes and the distribution of KSHV infection via GFP expression. Total GFP+ viable B lymphocytes represented as (A) raw percentages or (B) normalized to the untreated control for each tonsil sample. For (A) one-way repeated measures ANOVA shows p=0.00001, F=9.4 for the main effect of IL-21 neutralization and Dunnett's test reveals p=0.03 at the 100µg/ml dose. (C) frequencies of B cell subsets in the cultures. Red boxes indicate significant results as follows: Two-way repeated measures ANOVA on the raw data showed significant effects of IL-21 treatment on B subset frequencies; IgG+ (p=0.04, F=5.0), memory (p=0.03, F=3.4), and double negative (p=0.02, F=3.8), IgM+ (p=0.0003, F=8.6), transitional (p=0.01, F=4.1). Post-hoc paired T-tests showed significant effect of 200µg/ml

neutralizing antibody on total plasma cells (p=0.02) and CD20+ plasma cells (p=0.005) in Mock cultures only. (D) Effect of indicated doses of IL-21 neutralizing antibody on KSHV infection of B cell subsets. Data is normalized to each sample's untreated control level for each B cell subset. One-way repeated measures ANOVA on the raw data reveals a significant effect on infection of transitional B cells (p=0.01, F=4.0). (E) Correlation between the effect of IL-21 neutralization on overall infection (x-axis) and the contribution of each subset to KSHV infection in the same condition (y-axis). Shapes indicate doses in this panel (circle=100µg/ml, triangle=200µg/ml, square=400µg/ml). Subsets with statistically significant correlations are indicated by red boxes with statistics from Pearson's linear correlation as follows: CD20+ plasma cells (r=0.6, p=0.0002), plasma cells (r=0.6, p=0.0003), transitional (r=0.5, p=0.004), germinal center (r=-0.4, p=0.02). For panels C-E colors indicate unique tonsil specimens and can be compared between these panels and red diamonds indicate the mean value for all tonsil specimens. RT-PCR analysis of KSHV transcripts at 3 dpi in 8 unique tonsil specimens with either IL-21 supplementation at 100 pg/ml (Fig 2) or IL-21 neutralizing antibody at 100µg/ml with LANA (latent) and K8.1 (lytic) transcript targets. No RT controls were used to determine that RT-PCR signal is not due to DNA contamination (F) Cq values for viral targets normalized to the within-sample Cq for GAPDH (G) GAPDH-normalized values further normalized to the within-sample value for the untreated control.

Figure 4: IL21 receptor distribution in primary human tonsil B lymphocytes affects the magnitude and distribution of KSHV infection. B cell immunophenotyping analysis including IL-21R was performed at baseline (Day 0) for 10 unique tonsil specimens. (A) total percentage of IL-21R+ within viable CD19+ B cells. (B) Percent of individual B cell subsets within IL-21+ B cells. Red diamonds indicate the mean value for all tonsil specimens and (C) distribution of B cell

subsets within IL-21+ on a per-tonsil basis. (D) correlation analysis of baseline IL-21 receptor distribution within subsets and the overall susceptibility of the same tonsil specimen to KSHV infection at 3 dpi. Pearson correlation coefficients and p-values are denoted on panels where the result is statistically significant. (E) correlation analysis of baseline IL-21 receptor distribution with the effect of IL-21 supplementation on overall KSHV infection in the same tonsil specimens. Pearson correlation coefficients and p-values are denoted on panels where the result is statistically significant. (F) correlation analysis of baseline IL-21 receptor distribution with the IL-21 mediated increase in total plasma cell numbers at 3dpi in KSHV-infected cultures in the same tonsil specimens. (G) Distribution of IL-21 receptor at day 0 (baseline) or 3dpi within Mock, Mock+100ng/ml IL-21, KSHV or KSHV+ 100ng/ml IL-21 conditions. Red diamonds indicate the mean values for each condition and significant differences were assessed via paired T-test.

Figure 5: Characterization of T cell subsets producing IL-21 in primary human tonsil B lymphocytes. T cells were analyzed by surface immunophenotyping, intracellular transcription factor staining and ICCS for IL-21 secretion in Mock and KSHV-infected total lymphocyte cultures at 3 dpi in 14 unique tonsil specimens. (A) Total IL-21+ viable non-B cells (B) percent of CD4+ or CD8+ T cells within IL-21+. For (A) and (B) red diamonds indicate the mean value for the condition and colors indicate specific tonsil specimens and can be compared between the panels. (C) Immunophenotypic analysis of T cell subsets (Table 2) within IL-21+ in Mock (red) and KSHV (blue) cultures. (D) Data as in (C) but normalized to show the induction or repression of the T cell subset within IL-21+ cells (KSHV-Mock). *p=0.05; **p=0.04; ***p=0.003 comparing Mock and KSHV-infected via paired T test pre-normalization.

Figure 6: IL-21 secretion by CD8+ central memory T cells influences both overall KSHV infection and plasma cell targeting. Lymphocyte cultures from the experiments shown in Fig 5 were further analyzed for B cell subsets and the magnitude and distribution of KSHV infection. (A) correlation analysis of total GFP+ within viable, CD19+ B lymphocytes at 3 dpi with total IL-21 secretion in non-B cells or the contribution of individual T cell subsets to IL-21 secretion. Pearson's correlation coefficient and p-value is shown on panels that have statistically significant correlations. (B) correlogram of Pearson correlations between the distribution of KSHV infection within B cell subsets (y-axis) and total IL-21 or the contribution of individual T cell subsets to IL-21 secretion (x-axis). Pearson's r values with an absolute value greater than or equal to 0.53 are statistically significant for this dataset. (C) scatterplot and linear model fit for the correlation between GFP+ plasma cells and IL-21 secretion by CD8+ central memory T cells (D) Scatterplots and linear model fits for the correlations between GFP+ plasma cells and secretion of IL-21 by RoRγT+ CD4+ (left) or CD8+ (right) T cells. (E) correlogram of Pearson correlations between the distribution of KSHV infection within B cell subsets (y-axis) and baseline (Day 0) levels of T cell subsets. Pearson's r values with an absolute value greater than or equal to 0.53 are statistically significant for this dataset. (F) scatterplot and linear model fit for the correlation between GFP+ plasma cells and baseline frequency of CD8+ central memory T cells. For A, C, D and F grey shading indicates 95% confidence intervals.

Supplemental Figure 1: Representative gating scheme for T cell immunophenotyping using lineage definitions as detailed in Table 2.

Supplemental Figure 2: Total T cell subset frequencies in Mock and KSHV-infected cultures as in Figure 5.

References

1. Chang, Y., et al., *Identification of herpesvirus-like DNA sequences in AIDS-associated Kaposi's sarcoma.* Science, 1994. **266**(5192): p. 1865-1869.
2. Ablashi, D.V., et al., *Spectrum of Kaposi's sarcoma-associated herpesvirus, or human herpesvirus 8, diseases.* Clinical microbiology reviews, 2002. **15**(3): p. 439-464.
3. Cesarman, E., et al., *Kaposi's sarcoma–associated herpesvirus-like DNA sequences in AIDS-related body-cavity–based lymphomas.* New England Journal of Medicine, 1995. **332**(18): p. 1186-1191.
4. Soulier, J., et al., *Kaposi's sarcoma-associated herpesvirus-like DNA sequences in multicentric Castleman's disease [see comments].* Blood, 1995. **86**(4): p. 1276-1280.
5. Uldrick, T.S., et al., *An interleukin-6-related systemic inflammatory syndrome in patients co-infected with Kaposi sarcoma-associated herpesvirus and HIV but without Multicentric Castleman disease.* Clinical Infectious Diseases, 2010. **51**(3): p. 350-358.
6. Bouvard, V., et al., *A review of human carcinogens--Part B: biological agents.* The Lancet. Oncology, 2009. **10**(4): p. 321-322.
7. Parkin, D.M., *The global health burden of infection-associated cancers in the year 2002.* International journal of cancer, 2006. **118**(12): p. 3030-3044.
8. Ganem, D., *KSHV and the pathogenesis of Kaposi sarcoma: listening to human biology and medicine.* The Journal of clinical investigation, 2010. **120**(4): p. 939-949.
9. Casper, C., et al., *Frequent and asymptomatic oropharyngeal shedding of human herpesvirus 8 among immunocompetent men.* The Journal of infectious diseases, 2007. **195**(1): p. 30-36.
10. Alomari, N. and J. Totonchy, *Cytokine-Targeted Therapeutics for KSHV-Associated Disease.* Viruses, 2020. **12**(10): p. 1097.
11. Carbone, A., et al., *Understanding pathogenetic aspects and clinical presentation of primary effusion lymphoma (PEL) through its derived cell lines.* AIDS (London, England), 2010. **24**(4): p. 479.
12. Aalam, F., et al., *Analysis of KSHV B lymphocyte lineage tropism in human tonsil reveals efficient infection of CD138+ plasma cells.* PLoS pathogens, 2020. **16**(10): p. e1008968.
13. Parrish-Novak, J., et al., *Interleukin-21 and the IL-21 receptor: novel effectors of NK and T cell responses.* Journal of leukocyte biology, 2002. **72**(5): p. 856-863.
14. Parrish-Novak, J., et al., *Interleukin 21 and its receptor are involved in NK cell expansion and regulation of lymphocyte function.* Nature, 2000. **408**(6808): p. 57-63.
15. Kuchen, S., et al., *Essential role of IL-21 in B cell activation, expansion, and plasma cell generation during CD4+ T cell-B cell collaboration.* The journal of immunology, 2007. **179**(9): p. 5886-5896.
16. Konforte, D., N. Simard, and C.J. Paige, *IL-21: an executor of B cell fate.* The Journal of Immunology, 2009. **182**(4): p. 1781-1787.
17. Ozaki, K., et al., *Regulation of B cell differentiation and plasma cell generation by IL-21, a novel inducer of Blimp-1 and Bcl-6.* The Journal of Immunology, 2004. **173**(9): p. 5361-5371.

18. Calame, K.L., K.-I. Lin, and C. Tunyaplin, *Regulatory mechanisms that determine the development and function of plasma cells.* Annual review of immunology, 2003. **21**(1): p. 205-230.
19. Yajima, H., et al., *Loss of interleukin-21 leads to atrophic germinal centers in multicentric Castleman's disease.* Annals of hematology, 2016. **95**(1): p. 35-40.
20. Konforte, D. and C.J. Paige, *Identification of cellular intermediates and molecular pathways induced by IL-21 in human B cells.* The Journal of Immunology, 2006. **177**(12): p. 8381-8392.
21. Konforte, D., N. Simard, and C.J. Paige, *Interleukin-21 regulates expression of key Epstein–Barr virus oncoproteins, EBNA2 and LMP1, in infected human B cells.* Virology, 2008. **374**(1): p. 100-113.
22. Collins, C.M. and S.H. Speck, *Interleukin 21 signaling in B cells is required for efficient establishment of murine gammaherpesvirus latency.* PLoS pathogens, 2015. **11**(4): p. e1004831.
23. Gasperini, P. and G. Tosato, *Targeting the mammalian target of Rapamycin to inhibit VEGF and cytokines for the treatment of primary effusion lymphoma.* Leukemia, 2009. **23**(10): p. 1867-1874.
24. Gasperini, P., S. Sakakibara, and G. Tosato, *Contribution of viral and cellular cytokines to Kaposi's sarcoma-associated herpesvirus pathogenesis.* Journal of leukocyte biology, 2008. **84**(4): p. 994-1000.
25. Totonchy, J., et al., *KSHV induces immunoglobulin rearrangements in mature B lymphocytes.* PLoS pathogens, 2018. **14**(4): p. e1006967.
26. Chang, J., et al., *Induction of Kaposi's sarcoma-associated herpesvirus from latency by inflammatory cytokines.* Virology, 2000. **266**: p. 17-25.
27. Chang, J., et al., *Inflammatory cytokines and the reactivation of Kaposi's sarcoma-associated herpesvirus lytic replication.* Virology, 2000. **266**(1): p. 17-25.
28. Palmerin, N., et al., *Suppression of DC-SIGN and gH Reveals Complex, Subset-Specific Mechanisms for KSHV Entry in Primary B Lymphocytes. Viruses 2021, 13, 1512*. 2021, s Note: MDPI stays neutral with regard to jurisdictional claims in published ….
29. Schmitz, I., et al., *IL-21 restricts virus-driven Treg cell expansion in chronic LCMV infection.* PLoS pathogens, 2013. **9**(5): p. e1003362.
30. Pallikkuth, S., et al., *Upregulation of IL-21 receptor on B cells and IL-21 secretion distinguishes novel 2009 H1N1 vaccine responders from nonresponders among HIV-infected persons on combination antiretroviral therapy.* The Journal of Immunology, 2011. **186**(11): p. 6173-6181.
31. Jondle, C., et al., *Gammaherpesvirus Usurps Host IL-17 Signaling To Support the Establishment of Chronic Infection.* Mbio, 2021. **12**(2): p. e00566-21.
32. Jondle, C., et al., *T Cell-Intrinsic Interferon Regulatory Factor 1 Expression Suppresses Differentiation of CD4+ T Cell Populations That Support Chronic Gammaherpesvirus Infection.* Journal of Virology, 2021. **95**(20): p. e00726-21.
33. Gaddi, P.J. and G.S. Yap, *Cytokine regulation of immunopathology in toxoplasmosis.* Immunology and cell biology, 2007. **85**(2): p. 155-159.
34. Kelly, M.N., et al., *Interleukin-17/interleukin-17 receptor-mediated signaling is important for generation of an optimal polymorphonuclear response against Toxoplasma gondii infection.* Infection and immunity, 2005. **73**(1): p. 617-621.

35. Shainheit, M.G., et al., *The pathogenic Th17 cell response to major schistosome egg antigen is sequentially dependent on IL-23 and IL-1β.* The Journal of Immunology, 2011. **187**(10): p. 5328-5335.
36. Wen, X., et al., *Dynamics of Th17 cells and their role in Schistosoma japonicum infection in C57BL/6 mice.* PLoS neglected tropical diseases, 2011. **5**(11): p. e1399.
37. Wakeham, K., et al., *Parasite infection is associated with Kaposi's sarcoma associated herpesvirus (KSHV) in Ugandan women.* Infectious agents and cancer, 2011. **6**(1): p. 1-7.
38. Song, W. and J. Craft, *T follicular helper cell heterogeneity: time, space, and function.* Immunological reviews, 2019. **288**(1): p. 85-96.
39. Totonchy, J., *Extrafollicular activities: perspectives on HIV infection, germinal center-independent maturation pathways, and KSHV-mediated lymphoproliferation.* Current opinion in virology, 2017. **26**: p. 69-73.
40. Yang, R., et al., *IL-6 promotes the differentiation of a subset of naive CD8+ T cells into IL-21–producing B helper CD8+ T cells.* Journal of Experimental Medicine, 2016. **213**(11): p. 2281-2291.
41. Wickham, H., *Ggplot2 : elegant graphics for data analysis*. Use R! 2009, New York: Springer. viii, 212 p.
42. Kassambara, A., *ggcorrplot: Visualization of a Correlation Matrix using 'ggplot2'.* 2019.
43. Lander, J.P., *R for everyone : advanced analytics and graphics*. Second edition ed. The Addison Wesley data and anlytics series. 2017, Boston: Addison-Wesley. xxiv, 528 pages.
44. Kassambara, A., *rstatix: Pipe-Friendly Framework for Basic Statistical Tests.* 2020.

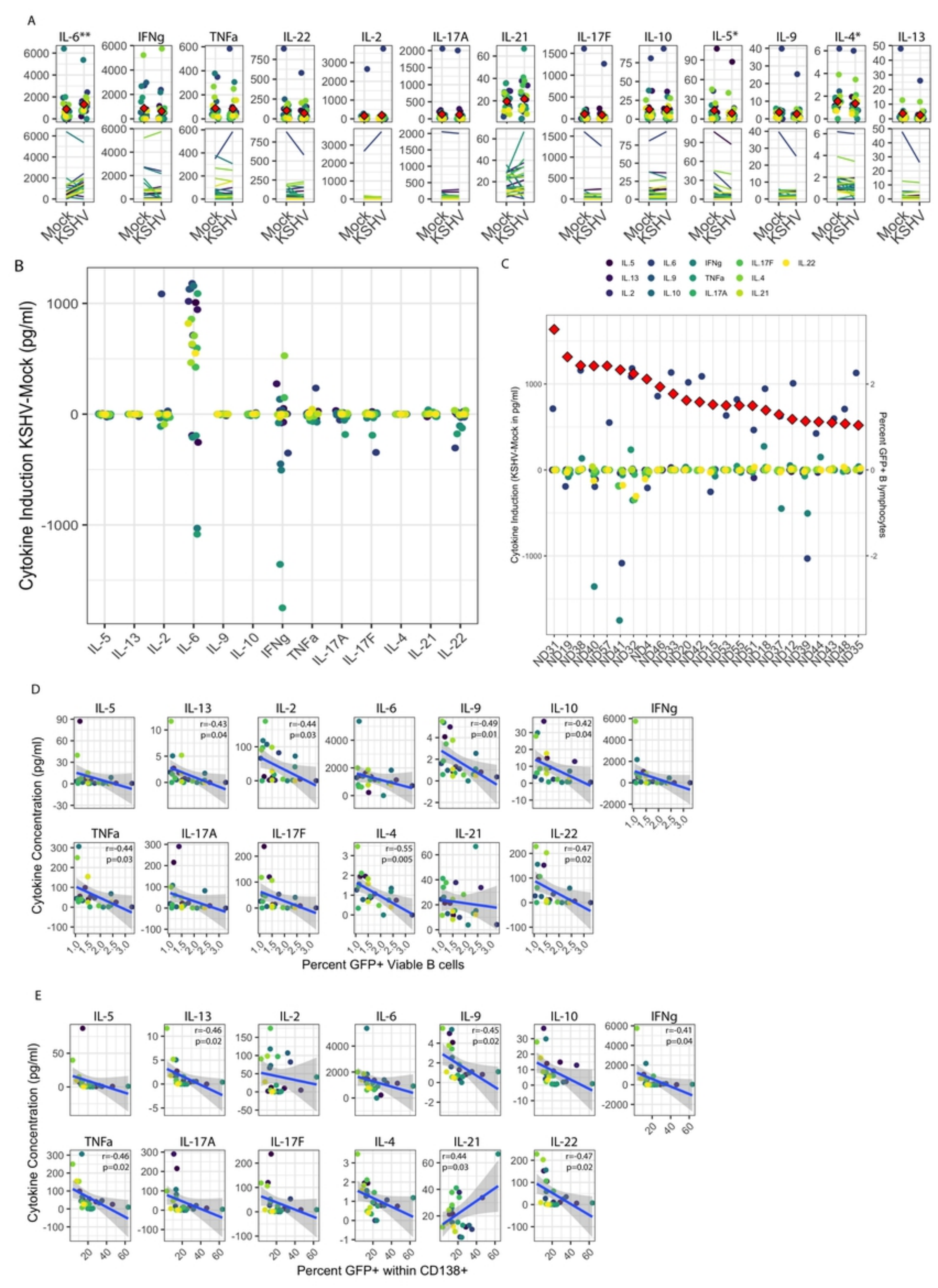
A
IL-6** IFNg TNFa IL-22 IL-2 IL-17A IL-21 IL-17F IL-10 IL-5* IL-9 IL-4* IL-13
Mock KSHV
B
Cytokine Induction KSHV-Mock (pg/ml)
IL-5 IL-13 IL-2 IL-6 IL-9 IL-10 IFNg TNFa IL-17A IL-17F IL-4 IL-21 IL-22
C
IL.5 IL.13 IL.2 IL.6 IL.9 IL.10 IFNg TNFa IL.17A IL.17F IL.4 IL.21 IL.22
Cytokine Induction (KSHV-Mock in pg/ml)
Percent GFP+ B lymphocytes
D
IL-5 IL-13 IL-2 IL-6 IL-9 IL-10 IFNg
r=-0.43 p=0.04
r=-0.44 p=0.03
r=-0.49 p=0.01
r=-0.42 p=0.04
TNFa IL-17A IL-17F IL-4 IL-21 IL-22
r=-0.44 p=0.03
r=-0.55 p=0.005
r=-0.47 p=0.02
Cytokine Concentration (pg/ml)
Percent GFP+ Viable B cells
E
IL-5 IL-13 IL-2 IL-6 IL-9 IL-10 IFNg
r=-0.46 p=0.02
r=-0.45 p=0.02
r=-0.41 p=0.04
TNFa IL-17A IL-17F IL-4 IL-21 IL-22
r=-0.46 p=0.02
r=0.44 p=0.03
r=-0.47 p=0.02
Cytokine Concentration (pg/ml)
Percent GFP+ within CD138+

Figure 1

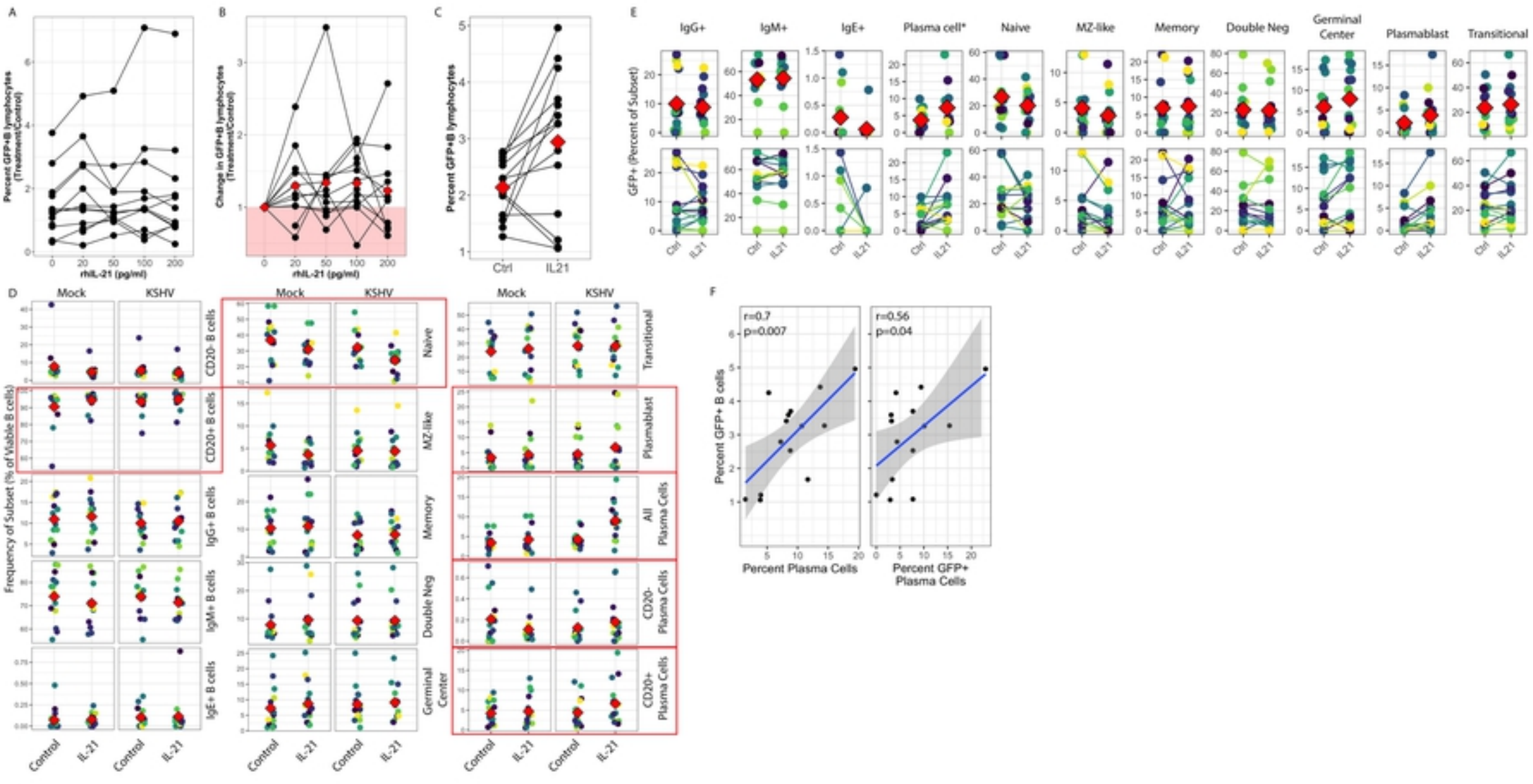
A
Percent GFP+B lymphocytes (Treatment/Control)
rhIL-21 (pg/ml)
B
Change in GFP+B lymphocytes (Treatment/Control)
rhIL-21 (pg/ml)
C
Percent GFP+B lymphocytes
Ctrl
IL21
E
IgG+
IgM+
IgE+
Plasma cell*
Naive
MZ-like
Memory
Double Neg
Germinal Center
Plasmablast
Transitional
GFP+ (Percent of Subset)
Ctrl
IL21
D
Mock
KSHV
CD20- B cells
CD20+ B cells
IgG+ B cells
IgM+ B cells
IgE+ B cells
Naive
MZ-like
Memory
Double Neg
Germinal Center
Transitional
Plasmablast
All Plasma Cells
CD20- Plasma Cells
CD20+ Plasma Cells
Frequency of Subset (% of Viable B cells)
Control
IL-21
F
r=0.7
p=0.007
r=0.56
p=0.04
Percent GFP+ B cells
Percent Plasma Cells
Percent GFP+ Plasma Cells

Figure 2

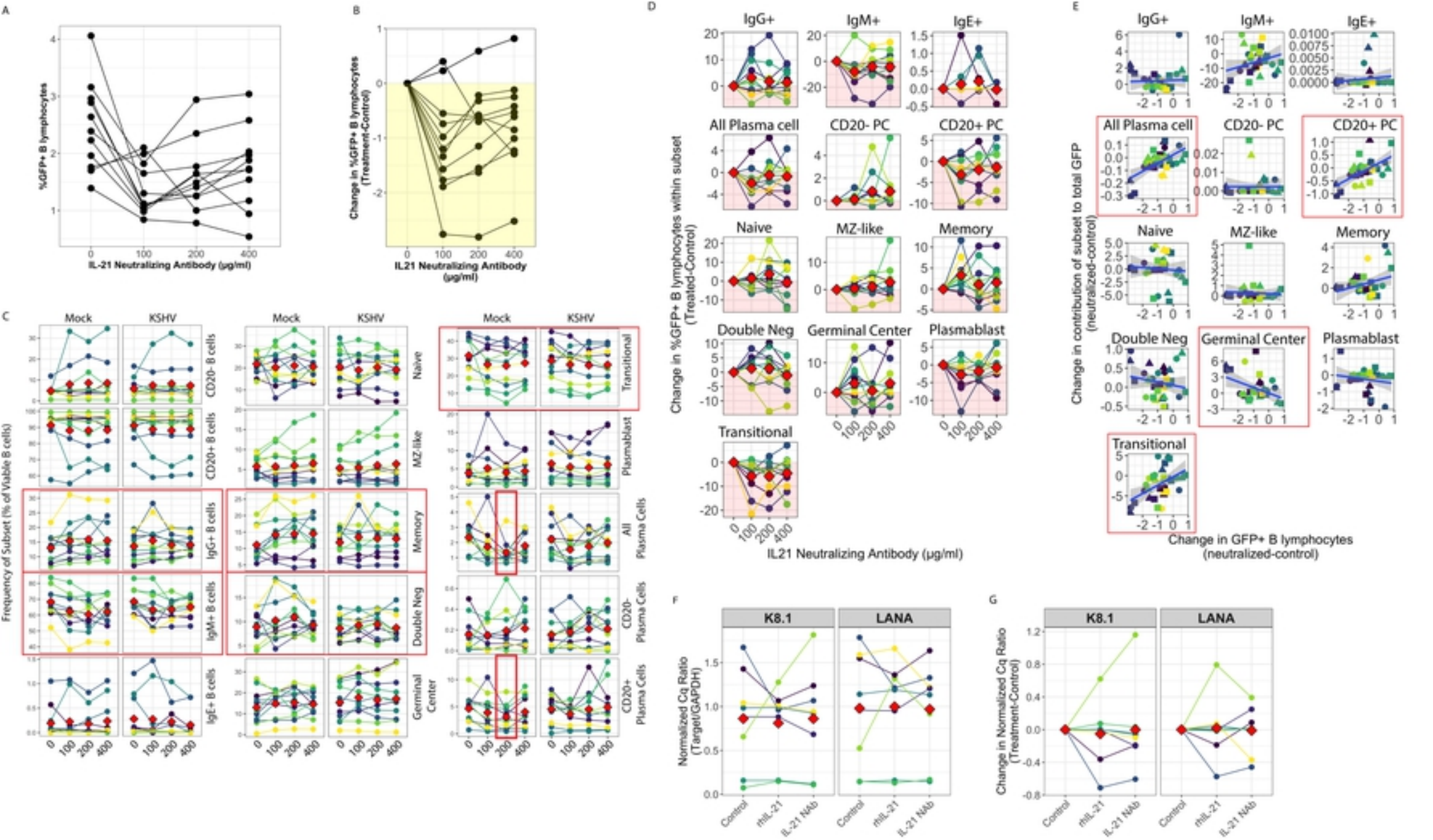
A
%GFP+ B lymphocytes
IL-21 Neutralizing Antibody (µg/ml)
B
Change in %GFP+ B lymphocytes (Treatment-Control)
IL21 Neutralizing Antibody (µg/ml)
C
Mock
KSHV
Frequency of Subset (% of Viable B cells)
CD20- B cells
CD20+ B cells
IgG+ B cells
IgM+ B cells
IgE+ B cells
Naive
MZ-like
Memory
Double Neg
Germinal Center
Transitional
Plasmablast
All Plasma Cells
CD20- Plasma Cells
CD20+ Plasma Cells
D
IgG+
IgM+
IgE+
All Plasma cell
CD20- PC
CD20+ PC
Naive
MZ-like
Memory
Double Neg
Germinal Center
Plasmablast
Transitional
Change in %GFP+ B lymphocytes within subset (Treated-Control)
IL21 Neutralizing Antibody (µg/ml)
E
Change in contribution of subset to total GFP (neutralized-control)
Change in GFP+ B lymphocytes (neutralized-control)
F
K8.1
LANA
Normalized Cq Ratio (Target/GAPDH)
Control
rhIL-21
IL-21 NAb
G
Change in Normalized Cq Ratio (Treatment-Control)

Figure 3

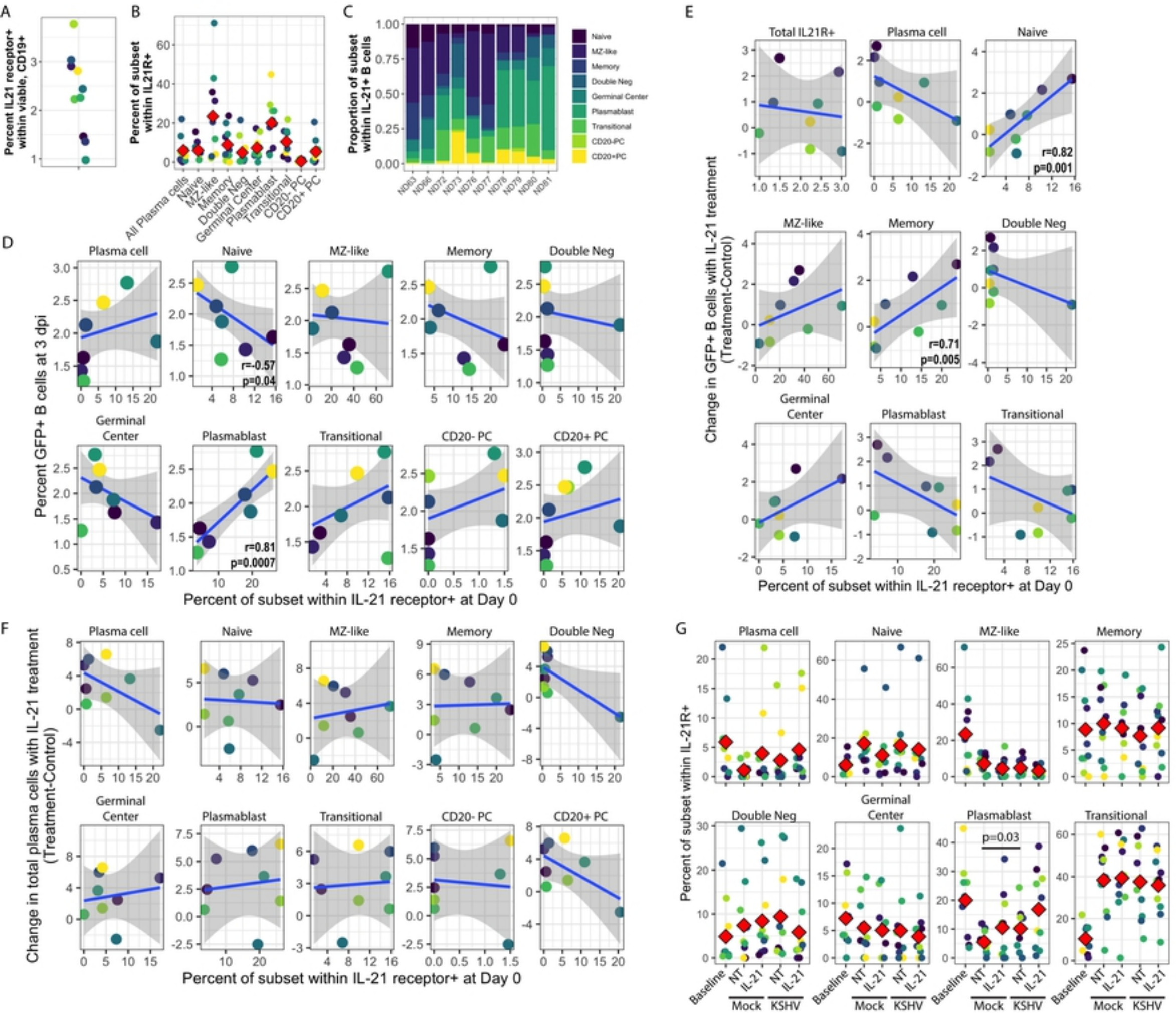
A
Percent IL21 receptor+ within viable, CD19+
B
Percent of subset within IL21R+
All Plasma cells
Naive
MZ-like
Memory
Double Neg
Germinal Center
Plasmablast
Transitional
CD20- PC
CD20+ PC
C
Proportion of subset within IL-21+ B cells
ND63
ND66
ND72
ND73
ND76
ND77
ND78
ND79
ND80
ND81
Naive
MZ-like
Memory
Double Neg
Germinal Center
Plasmablast
Transitional
CD20-PC
CD20+PC
D
Percent GFP+ B cells at 3 dpi
Plasma cell
Naive
r=-0.57
p=0.04
MZ-like
Memory
Double Neg
Germinal Center
Plasmablast
r=0.81
p=0.0007
Transitional
CD20- PC
CD20+ PC
Percent of subset within IL-21 receptor+ at Day 0
E
Change in GFP+ B cells with IL-21 treatment (Treatment-Control)
Total IL21R+
Plasma cell
Naive
r=0.82
p=0.001
MZ-like
Memory
r=0.71
p=0.005
Double Neg
Germinal Center
Plasmablast
Transitional
Percent of subset within IL-21 receptor+ at Day 0
F
Change in total plasma cells with IL-21 treatment (Treatment-Control)
Plasma cell
Naive
MZ-like
Memory
Double Neg
Germinal Center
Plasmablast
Transitional
CD20- PC
CD20+ PC
Percent of subset within IL-21 receptor+ at Day 0
G
Percent of subset within IL-21R+
Plasma cell
Naive
MZ-like
Memory
Double Neg
Germinal Center
Plasmablast
p=0.03
Transitional
Baseline
NT
IL-21
Mock
KSHV

Figure 4

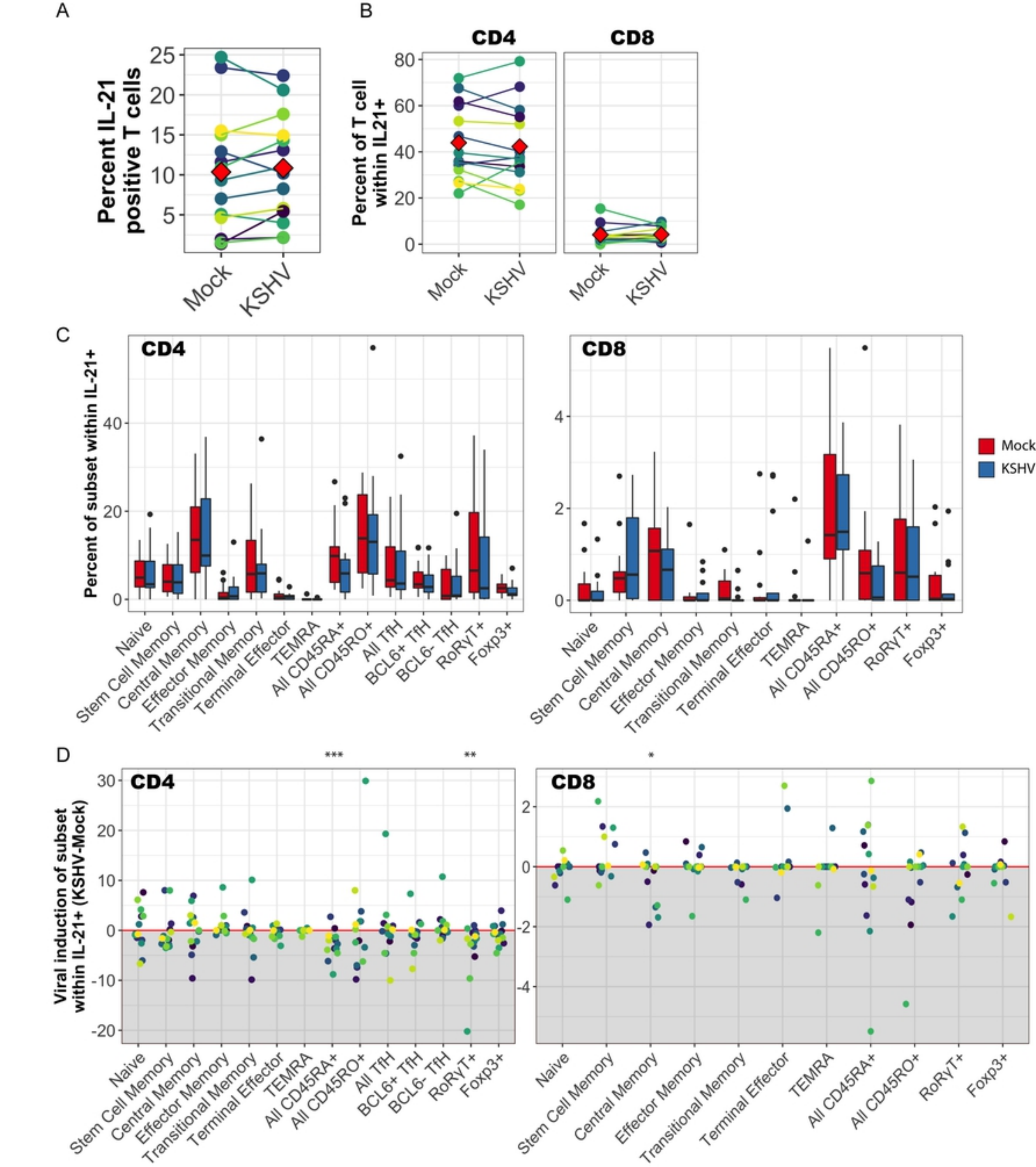
A
Percent IL-21 positive T cells
Mock
KSHV
B
CD4
CD8
Percent of T cell within IL21+
C
CD4
CD8
Percent of subset within IL-21+
Mock
KSHV
Naive
Stem Cell Memory
Central Memory
Effector Memory
Transitional Memory
Terminal Effector
TEMRA
All CD45RA+
All CD45RO+
All TfH
BCL6+ TfH
BCL6- TfH
RoRγT+
Foxp3+
D
CD4
CD8
Viral induction of subset within IL-21+ (KSHV-Mock)

Figure 5

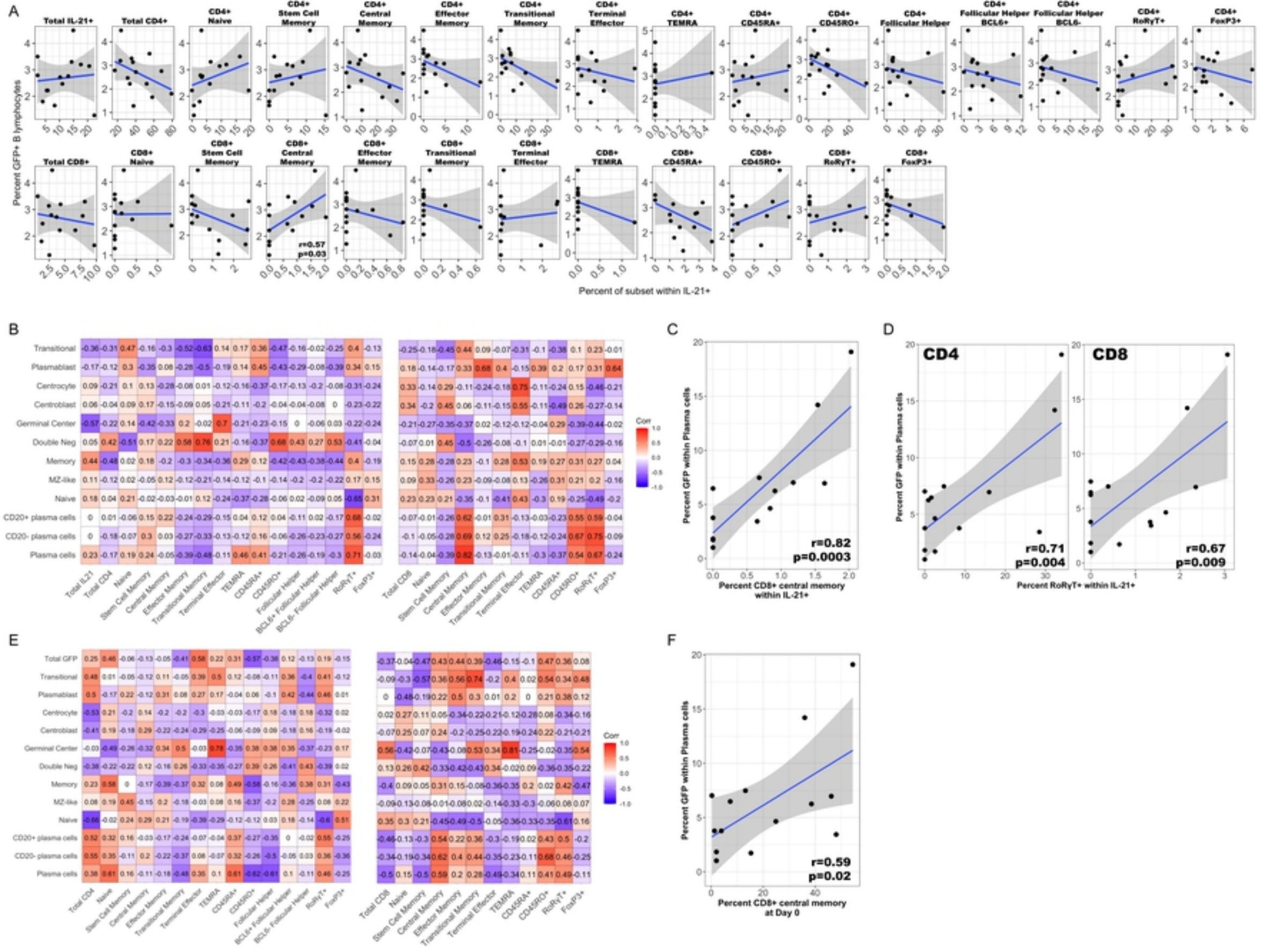
A
Total IL-21+
Total CD4+
CD4+ Naive
CD4+ Stem Cell Memory
CD4+ Central Memory
CD4+ Effector Memory
CD4+ Transitional Memory
CD4+ Terminal Effector
CD4+ TEMRA
CD4+ CD45RA+
CD4+ CD45RO+
CD4+ Follicular Helper
CD4+ Follicular Helper BCL6+
CD4+ Follicular Helper BCL6-
CD4+ RoRγT+
CD4+ FoxP3+
Total CD8+
CD8+ Naive
CD8+ Stem Cell Memory
CD8+ Central Memory
r=0.57
p=0.03
CD8+ Effector Memory
CD8+ Transitional Memory
CD8+ Terminal Effector
CD8+ TEMRA
CD8+ CD45RA+
CD8+ CD45RO+
CD8+ RoRγT+
CD8+ FoxP3+
Percent GFP+ B lymphocytes
Percent of subset within IL-21+
B
Transitional
Plasmablast
Centrocyte
Centroblast
Germinal Center
Double Neg
Memory
MZ-like
Naive
CD20+ plasma cells
CD20- plasma cells
Plasma cells
Total IL21
Total CD4
Total CD8
Stem Cell Memory
Central Memory
Effector Memory
Transitional Memory
Terminal Effector
TEMRA
CD45RA+
CD45RO+
Follicular Helper
BCL6+ Follicular Helper
BCL6- Follicular Helper
RoRγT+
FoxP3+
Corr
C
Percent GFP within Plasma cells
Percent CD8+ central memory within IL-21+
r=0.82
p=0.0003
D
CD4
CD8
Percent GFP within Plasma cells
Percent RoRγT+ within IL-21+
r=0.71
p=0.004
r=0.67
p=0.009
E
Total GFP
Transitional
Plasmablast
Centrocyte
Centroblast
Germinal Center
Double Neg
Memory
MZ-like
Naive
CD20+ plasma cells
CD20- plasma cells
Plasma cells
Total CD4
Total CD8
Stem Cell Memory
Central Memory
Effector Memory
Transitional Memory
Terminal Effector
TEMRA
CD45RA+
CD45RO+
Follicular Helper
BCL6+ Follicular Helper
BCL6- Follicular Helper
RoRγT+
FoxP3+
Corr
F
Percent GFP within Plasma cells
Percent CD8+ central memory at Day 0
r=0.59
p=0.02

Figure 6